International Journal of Heat and Mass Transfer 52 (2009) 1053–1057

Contents lists available at ScienceDirect

International Journal of Heat and Mass Transfer

journal homepage: www.elsevier.com/locate/ijhmt

Heat transfer enhancement by flow-induced vibration in heat exchangers

L. Cheng *, T. Luan, W. Du, M. Xu

Institute of Thermal Science and Technology, Shandong University, Jinan 250061, China

ARTICLE INFO

Article history:
Received 20 October 2006
Received in revised form 12 December 2007
Available online 7 September 2008

Keywords:
Heat exchanger
Flow-induced vibration
Heat transfer enhancement

ABSTRACT

The flow-induced vibration in heat exchanger is usually considered as a detrimental factor for causing the heat exchanger damage and is strictly prevented from its occurrence. Its positive role for the possible heat transfer enhancement has been neglected. In this article a novel approach is proposed to enhance the heat transfer by using the flow-induced vibration of a new designed heat transfer device. Thus the flow-induced vibration is effectively utilized instead of strictly avoiding it in the heat exchanger design. A heat exchanger is constructed with the new designed heat transfer devices. The vibration and the heat transfer of these devices are studied numerically and experimentally, and the correlation of the shell-side convective heat transfer coefficient is obtained. It is found that the new designed heat exchanger can significantly increase the convective heat transfer coefficient and decrease the fouling resistance. Therefore, a lasting heat transfer enhancement by the flow-induced vibration can be achieved.

1. Introduction

In heat exchangers, especially shell-and-tube heat exchangers, the flow-induced vibration can damage the heat transfer devices and tubes, and generate noise. Much effort has been devoted to the study of the influence of the shell-side flow on the vibration of the heat transfer devices. Weaver and Fitzpatrick [1] studied the vibration problems induced by the shell-side single phase flow in shell-and-tube heat exchangers and proposed the preventive approaches against the tube bundle damage caused by the vibration. Pettigrew and Taylor [2] reviewed the main mechanisms of vibration induced by the two-phase flow and the impacts of dynamic parameters on the tube vibration. They revealed the damping properties of the shell-and-tube heat exchanger vibration induced by the two-phase flow by using a semi-empirical formula, and established a practical design criterion by integrating the dynamic parameters related to the damping into the empirical formula [3]. The flow-induced vibration problems in spiral finned gas tube bundle heat exchangers were studied by Michael [4]. After modified with both static and dynamic experimental results, a theoretical computational method, which normally uses for calculation of the natural frequencies of ordinary tubes, was used to handle the spiral-fin tube case, and some case studies regarding the damages caused by the fluid elastic instability in the spiral-fin tube heat exchanger were carried out. The vibration of the double 90° U-tubes used frequently in the steam generators for nuclear reactors was studied by Choi et al. [5]. They believed that when the shell-side flow velocity does not reach the critical value but is near the sub-critical value, the turbulence-induced vibration is the main cause for the vibration damages. A theoretical analysis model for the double 90° U-tubes was established based on the theoretical analysis model for the equal spacing straight tube, and was corrected further by the experimental data. The analysis model was used to predict the vibration-induced abrasion for the bent tubes in steam generators. A computational method for the shell-side critical velocity with non-equidistance nonlinear supports was reported by Au-Yang and Burgess [6], which provided the theoretical basis for precisely predicting the occurrence of the flow-induced vibration. The new type of heat exchanger with rod baffles developed for preventing from the flow-induced vibration was described in Ref. [7]. In order to protect the heat exchanger from vibration-induced damage, the supports to the heat transfer tubes were strengthened by changing the structures of the circular plate baffles [8]. Helical baffles were employed to change the shell-side velocity field, which not only mitigate the vibration-induced damage, but also enhance the heat transfer [9]. The fact, however, is that the design method for appropriately addressing the flow-induced vibration problems in heat exchangers has not been well-developed yet.

The essence of vibration is that the mechanical energy continuously accumulates and dissipates. The flow of media in the heat exchanger may cause the energy buildup due to the fluid viscosity. Therefore, it is almost impossible to completely avoid the vibration of the heat transfer devices. It is not always an effective approach to prevent heat transfer devices from the vibration by increasing the strength of the devices. Sometime it may be better to dissipate the energy by the limited vibration to prevent the devices from damage and avoid noise caused by the strong vibration. If we can find a way to induce the heat transfer device vibration, which

* Corresponding author. Tel.: +86 531 88399000; fax: +86 531 88399598.
E-mail address: cheng@sdu.edu.cn (L. Cheng).

0017-9310/$ - see front matter © 2008 Published by Elsevier Ltd.
doi:10.1016/j.ijheatmasstransfer.2008.05.037

Nomenclature

c_p	specific heat at constant pressure, J/kg K	R	radius of curvature of the curved tube, m
d	diameter of heat transfer tube, m	t''_f	outlet temperature of fluid, °C
F	heat transfer area, m^2	t'_f	inlet temperature of fluid, °C
M	additional mass, kg	t'_W	wall temperature, °C
$\dot{m}$	mass flow rate, kg/s	α	convective heat transfer coefficient, W/m^2 K
Nu	Nusselt number	δ	wall thickness, m
Pr	Prandtl number	ρ	fluid density, kg/m^3
Pr_f	Prandtl number at fluid average temperature	Δt	temperature difference, °C
Pr_w	Prandtl number at wall temperature		
Q	heat transfer rate, W		
Re	Reynolds number		

can be controlled by adjusting its damping to avoid the occurrence of vibration-induced damage, then the flow-induced vibration may be beneficial to the heat transfer. This article presents a new approach to enhance the heat transfer by the flow-induced vibration. The convective heat transfer coefficient is increased significantly for low velocity cases. Furthermore, the fouling problem on the heat transfer surface can be related to the flow-induced vibration, namely, the flow-induced vibration can be employed to restrain the fouling, thus reduce the fouling resistance. The heat transfer device used here is quite different from the normal one. It is an elastic tube bundle consisting of the coupled curved beams. The theoretical analysis and experimental study about the vibration and heat transfer of this new heat transfer device is performed, a novel approach to enhance heat transfer by the flow-induced vibration is established.

2. The structure of the new heat transfer device

In fact, a weak vibration of the heat transfer device always occurs when the fluid flows in a shell-and-tube heat exchanger. This weak vibration will neither cause the vibration-induced damage nor apparently impact on the heat transfer. Although many theoretical and empirical formulas are available for predicting the possibility of the occurrence of the flow-induced vibration, the fact is that the flow-induced vibration always occurs randomly. Therefore, to avoid such vibration encounter the same difficulty as to use it. In the present work we attempt to seek a new type of heat transfer device, which can freely vibrate under the influence of the fluid flows, and dissipate some energy through the continuous limited vibration, thus avoid the violent vibration, meanwhile it enhances the heat transfer by the continuous disturbance exerted on the flow by the vibration.

Both the structure and the arrangement of the new heat transfer device in the heat exchanger are different from the conventional one. It exhibits complex nonlinear features. The main structure of this device is a tube bundle which consists of four circular copper tubes with different radius of curvature as shown in Fig. 1. There are two solid joint bodies in points E and F. Both of them have additional masses and can freely vibrate. Their function is to adjust the natural frequencies of the tube bundle, in the same time they can serve as expanding joints. The points I and II are the clamped ends. They are connected with the inlet and the outlet of the heat exchanger standpipe, respectively. The hot medium flows into the heat transfer tubes from point I and out from the point II after releasing the heat. The heat transfer devices are arranged layer by layer as horizontal cantilevers. By adjusting the parameters of the radius of circular tube curvature R, the tube diameter d, the tube thickness δ and the additional masses of the solid bodies at points E and F, an appropriate natural frequency could be obtained, and thus the vibration with a desired magnitude could be induced by the pulsation in the flow process, which would be of benefit to the heat transfer in the heat exchanger.

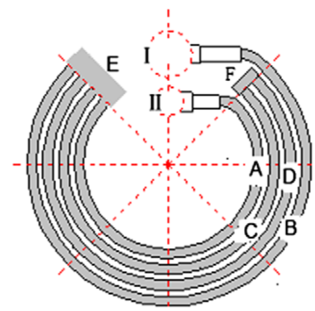

Fig. 1. The sketch of the nonlinear heat transfer device.

3. Vibration analysis

Since the shape of the nonlinear heat transfer device as shown in Fig. 1 is not regular, the dynamic sub-structure method is applied to its vibration analysis. According to its structure feature, it can be divided into six sub-structures: four curved beams denoted as A, B, C and D for the copper tubes, two solid bodies denoted as E and F for the joint bodies. On the interface between the solid body E and the curved beams, there are four nodes denoted as 1, 2, 3 and 4, the solid body F is connected to the curved beams by nodes 5 and 6. The coordinates at the interface nodes are set to $\{u_i\}$ ($i = 1, 2, 3, \ldots, 6$).

Following the sub-structure synthesis method, the vibration governing equations of the curved beams A, B, C and D in the modal coordinate system are written as

$$[\bar{\boldsymbol{m}}_A]\begin{Bmatrix} \ddot{p}_{iA} \\ \ddot{\boldsymbol{u}}_1 \end{Bmatrix} + [\bar{k}_A]\begin{Bmatrix} p_{iA} \\ \boldsymbol{u}_1 \end{Bmatrix} = \begin{Bmatrix} 0 \\ \boldsymbol{f}_1 \end{Bmatrix} \tag{1}$$

$$[\bar{\boldsymbol{m}}_B]\begin{Bmatrix} \ddot{p}_{iB} \\ \ddot{\boldsymbol{u}}_2 \end{Bmatrix} + [\bar{k}_B]\begin{Bmatrix} p_{iB} \\ \boldsymbol{u}_2 \end{Bmatrix} = \begin{Bmatrix} 0 \\ \boldsymbol{f}_2 \end{Bmatrix} \tag{2}$$

$$[\bar{\boldsymbol{m}}_C]\begin{Bmatrix} \ddot{p}_{iC} \\ \ddot{\boldsymbol{u}}_3 \\ \ddot{\boldsymbol{u}}_5 \end{Bmatrix} + [\bar{k}_C]\begin{Bmatrix} p_{iC} \\ \ddot{\boldsymbol{u}}_3 \\ \ddot{\boldsymbol{u}}_5 \end{Bmatrix} = \begin{Bmatrix} 0 \\ \boldsymbol{f}_3 \\ \boldsymbol{f}_5 \end{Bmatrix} \tag{3}$$

$$[\bar{\boldsymbol{m}}_D]\begin{Bmatrix} \ddot{p}_{iD} \\ \ddot{\boldsymbol{u}}_4 \\ \ddot{\boldsymbol{u}}_6 \end{Bmatrix} + [\bar{k}_D]\begin{Bmatrix} p_{iD} \\ \ddot{\boldsymbol{u}}_4 \\ \ddot{\boldsymbol{u}}_6 \end{Bmatrix} = \begin{Bmatrix} 0 \\ \boldsymbol{f}_4 \\ \boldsymbol{f}_6 \end{Bmatrix} \tag{4}$$

where $[\bar{\boldsymbol{m}}_i]$ and $[\bar{\boldsymbol{k}}_i]$ (i = A, B, C, D) are the mass and stiffness matrixes of the curved beams in the modal coordinate system, $\{f_i\}$ ($i = 1, 2, \ldots, 6$) are the interface forces, $\{P_{iA}\}$, $\{P_{iB}\}$, $\{P_{iC}\}$ and $\{P_{iD}\}$ are the modal coordinate vectors. When the joint bodies are treated as solid bodies, the coordinates $\{u_1\}$, $\{u_2\}$, $\{u_3\}$ and $\{u_4\}$ at the interface nodes are not independent. Similarly, $\{u_5\}$ and $\{u_6\}$ are not independent either. If $\{u_1\}$ and $\{u_5\}$ are taken as the independent variables, we have the following transformations

$$\begin{bmatrix} \boldsymbol{u}_1 \\ \boldsymbol{u}_2 \\ \boldsymbol{u}_3 \\ \boldsymbol{u}_4 \end{bmatrix} = \begin{bmatrix} \boldsymbol{I} \\ \boldsymbol{\varphi}_2 \\ \boldsymbol{\varphi}_3 \\ \boldsymbol{\varphi}_4 \end{bmatrix} \boldsymbol{u}_1 = \boldsymbol{\varphi}_E \boldsymbol{u}_1 \tag{5}$$

$$\begin{bmatrix} \boldsymbol{u}_5 \\ \boldsymbol{u}_6 \end{bmatrix} = \begin{bmatrix} \boldsymbol{I} \\ \boldsymbol{\varphi}_6 \end{bmatrix} \boldsymbol{u}_5 = \boldsymbol{\varphi}_F \boldsymbol{u}_5 \tag{6}$$

The vibration governing equations of the two solid bodies in the physical coordinate system is

$$\boldsymbol{m}_E \begin{bmatrix} \ddot{\boldsymbol{u}}_1 \\ \ddot{\boldsymbol{u}}_2 \\ \ddot{\boldsymbol{u}}_3 \\ \ddot{\boldsymbol{u}}_4 \end{bmatrix} = \begin{bmatrix} -\boldsymbol{f}_1 \\ -\boldsymbol{f}_2 \\ -\boldsymbol{f}_3 \\ -\boldsymbol{f}_4 \end{bmatrix} \tag{7}$$

$$\boldsymbol{m}_F \begin{bmatrix} \ddot{\boldsymbol{u}}_5 \\ \ddot{\boldsymbol{u}}_6 \end{bmatrix} = \begin{bmatrix} -\boldsymbol{f}_5 \\ -\boldsymbol{f}_6 \end{bmatrix} \tag{8}$$

Instituting Eqs. (5) and (6) into Eqs. (7) and (8) and multiplying both sides of the resulting equations by $\boldsymbol{\varphi}_E^T$ and $\boldsymbol{\varphi}_F^T$, respectively, yield

$$\bar{\boldsymbol{m}}_E \boldsymbol{u}_1 = \boldsymbol{f}_E \tag{9}$$

$$\bar{\boldsymbol{m}}_F \boldsymbol{u}_5 = \boldsymbol{f}_F \tag{10}$$

where $\bar{\boldsymbol{m}}_E = \boldsymbol{\varphi}_E^T \boldsymbol{m}_E \boldsymbol{\varphi}_E$, $\bar{\boldsymbol{m}}_F = \boldsymbol{\varphi}_F^T \boldsymbol{m}_F \boldsymbol{\varphi}_F$,

$$\boldsymbol{f}_E = -(\boldsymbol{f}_1 + \boldsymbol{\varphi}_2^T \boldsymbol{f}_2 + \boldsymbol{\varphi}_3^T \boldsymbol{f}_3 + \boldsymbol{\varphi}_4^T \boldsymbol{f}_4),$$

$$\boldsymbol{f}_F = -(\boldsymbol{f}_5 + \boldsymbol{\varphi}_6^T \boldsymbol{f}_6).$$

Combining Eqs. (1)–(4) with (9) and (10) and eliminating the dependent generalized modal coordinates by the continuous conditions on the interface, we obtain the following free vibration equations of the tube bundle in the modal coordinate system,

$$\boldsymbol{m}\ddot{\boldsymbol{q}} + \boldsymbol{K}\boldsymbol{q} = \boldsymbol{0} \tag{11}$$

where $\boldsymbol{q}$ is the independent generalized modal coordinate vector, $\boldsymbol{m}$ and $\boldsymbol{k}$ are the mass and stiffness matrixes of the tube bundle, respectively.

The natural frequencies and mode shapes of the considered device are obtained by solving the characteristic equation of Eq. (11). The application of the above method on the heat transfer device leads to the first six natural frequencies and mode shapes, which are documented in Table 1. From this table, one can see that the vibration of the heat transfer device is not limited to the in-plane vibration which refers to the vibration in the plane of the tube bundle, but there also exists complex vibrations in the other directions. In the heat exchanger constructed by these heat transfer devices, the interaction of this three-dimensional vibration with the working fluid outside the tubes plays a very important role for improving the heat transfer performance and reducing the fouling resistance.

Table 1
The first six natural frequencies and mode shapes of the nonlinear heat transfer device

Order	Natural frequencies and modal shapes	Order	Natural frequencies and modal shapes
1	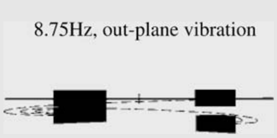	2	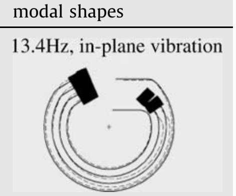
3	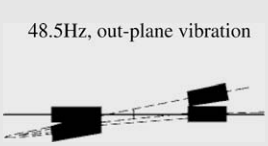	4	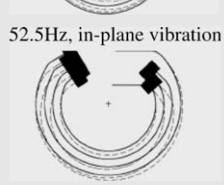
5	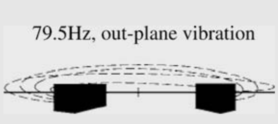	6	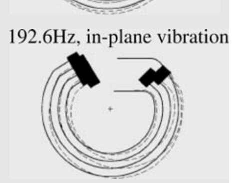

4. Heat transfer experiment

In order to study the heat transfer characteristics of the heat exchanger consisting of the nonlinear heat transfer devices, the heat transfer experiment is conducted under the constant heat flow condition. The constant heat flow condition is achieved by the electric heating inside the heat transfer tubes. The variation of the convective heat transfer coefficient outside the heat transfer tubes with the flow rate is investigated. In order to exhibit the effect of the heat enhancement by the flow-induced vibration, the experimental convective heat transfer coefficient is compared with that of the fixed bare tube for the same shell-side velocity. At the same time, the feature of the fouling resistance is experimentally studied.

The constant heat flow experiment system consists of the test part, water circulating system, electric heating system and the data collection system, as shown in Fig. 2. The test part is the heat exchanger constructed by the nonlinear heat transfer devices. In the water circulating system, the cold water from the water tank enters to the cycling pump via the filter, and then goes through the regulating valve and the flowmeter, and finally flows into the heat exchanger. After the heated water in the heat exchanger is cooled down, it flows back to the water tank. The nickel chromium resistance wire uniformly arranged inside the nonlinear heat transfer devices is employed to get the constant heat flow condition. The electric heating wire is drawn out from the inlet of tube 1 and the outlet of tube 2, respectively. The wire goes through the transformer, and is connected to the AC source with the voltage 220 v. The heating power can be changed by adjusting the voltage of the transformer. Its value can be obtained by the power meter. The inlet and the outlet temperatures of the heat exchanger can be measured by Φ 0.2 mm copper-constantan thermoelectric couples, which are verified by the standard thermometer with the accuracy 0.1 °C. The wall temperature of the nonlinear heat transfer device is also measured by copper-constantan thermoelectric couples. All the temperature signals are handled by the FLUKE data collection instrument. The inlet and the outlet pressures of the heat exchanger are measured by an elastic spring tube pressure gauge in order to obtain the flow friction of the working fluid outside the tube.

The steady heat flow method is employed to measure the convective heat transfer coefficient outside the nonlinear heat transfer device. Based on Newton's law of cooling:

$$\alpha = \frac{Q}{F\Delta t} = \frac{Q}{F(\bar{t}_w - \bar{t}_f)} \tag{12}$$

where α is the convective heat transfer coefficient, Q is the heat transfer rate, F is the heat transfer surface area, and

$$\bar{t}_w = \frac{1}{28} \sum_{i=1}^{28} t_{w,i} \tag{13}$$

$$\bar{t}_f = \frac{1}{2}(t''_f + t'_f) \tag{14}$$

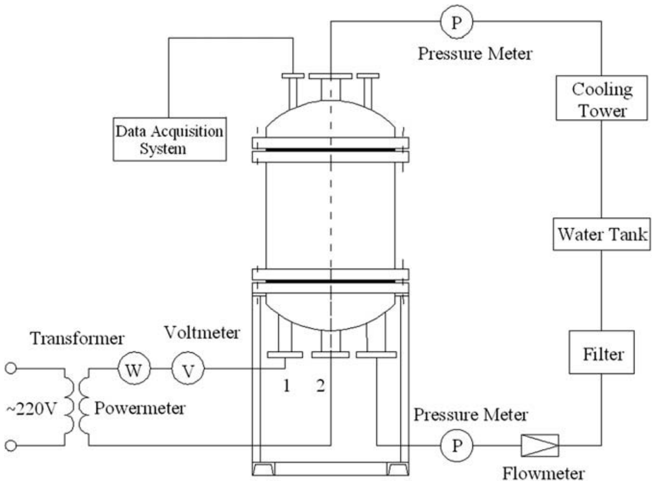

Fig. 2. The sketch of the experiment apparatus.

where $\bar{t}_w$ is the average temperature on the circular tube wall surface, $t_{w,i}$ ($i = 1,2,3,\ldots,28$) are the temperatures at uniformly distributed 28 points on the wall surface, and they are measured by the thermoelectric couples, t'_f and t''_f are the inlet and the outlet temperatures which are directly measured by the thermoelectric couples located in the inlet and the outlet of the tube. Under the adiabatic condition, the heat transfer rate is given as follows:

$$Q = c_p\dot{m}(t''_f - t'_f) \tag{15}$$

where c_p is the specific heat of fluid at constant pressure, $\dot{m}$ is the mass flow rate.

By using the computational method given in Ref. [10] and changing the inlet velocity of water, we can obtain the variations of the heat transfer coefficients outside the fixed single tube, the bottom tube bundle and the top tube bundle with respect to *Re* (Reynolds number), as shown in Fig. 3. It is found that since the cold water enters into the heat exchanger from the bottom and goes out from the top, the vibration induced by the flow pulsation occurs firstly in the bottom tube bundle. Therefore, this part demonstrates better heat transfer. With the water flowing upward, the pulsation-induced vibration becomes weak, and subsequently the heat transfer enhancement effect becomes worse, which means that the convective heat transfer coefficient outside of the tube is also decreased. In Fig. 3, only the convective heat transfer coefficients of the bottom and the top bundles are depicted, and the convective heat transfer coefficients of the middle tube bundles are between these two values. Although the heat transfer coefficient of the top bundle is decreased somewhat in comparison with the bottom bundle, they are all enhanced significantly than the fixed tube bundle without the flow-induced vibration.

In the present work the following formula is used for the data fitting process

$$Nu = CRe^m \mathrm{Pr}_f^{1/3}(\mathrm{Pr}_f/\mathrm{Pr}_w)^{0.25} \tag{16}$$

where C is a constant to be determined, *Nu* is the Nusselt number, *Re* is the Reynolds number, *Pr* is the Prantdl number, subscripts f and w refer to the fluid and wall, respectively. More reasonably the algebraic average of the convective heat convection coefficients of the top bundle and bottom bundle may be taken as the convective heat transfer coefficient outside the heat transfer tube. The data fitting process leads to the following correlation:

$$Nu = 0.9Re^{0.6}\mathrm{Pr}_f^{1/3}\left(\frac{\mathrm{Pr}_f}{\mathrm{Pr}_w}\right)^{0.25} \tag{17}$$

The comparison of the results obtained by Eq. (17) with the experimental results shows a good agreement, and the errors are normally within ±5%.

Note that the above expression of the convective heat transfer coefficient under the constant heat flow condition may not completely represent the heat transfer enhancement at the normal working condition. This is because only the tube outside vibration caused by the flow pulsation is considered in this experiment, and there is no tube inside vibration since there is no working fluid inside the tubes. In fact, the inside tube flow can also enhance the heat transfer in the heat exchanger under the normal working condition. The heat transfer performance of the heat exchanger under the combining actions of the tube inside and outside flow-induced vibration is much better than that in this experiment. We have also carried out the experimental study of the heat transfer in the nonlinear heat transfer device with the steam as the heat source so that the temperature on the surface of the wall can be kept constant. We obtained the variations of the convective heat transfer coefficients inside and outside the nonlinear heat transfer device with respect to the steam pressure and flow rate outside the tube. The details will be reported in another paper.

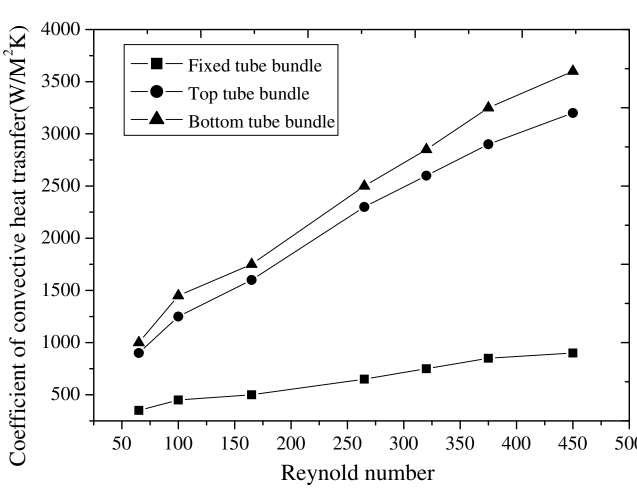

Fig. 3. Variation of the convective heat transfer coefficients with Re for different heat transfer tubes.

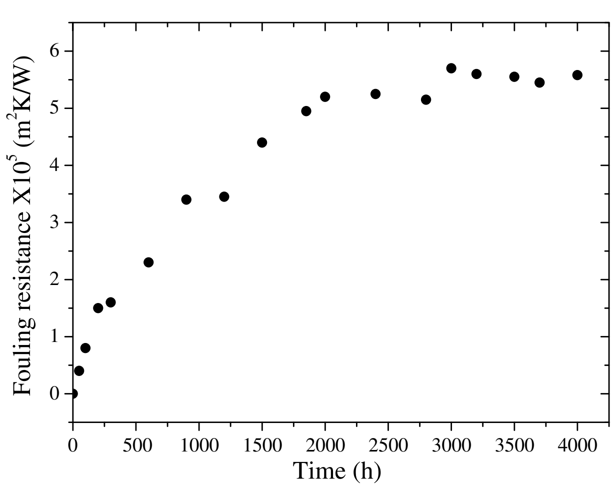

Fig. 4. Variation of the fouling resistance with time.

5. Fouling properties

The utilization of this heat transfer device not only enhances the heat transfer by the flow-induced vibration, but also decreases the fouling resistance outside the tubes. Although the mechanism that the vibration can get rid of the fouling is not completely clear, it is generally believed that the in-plane vibration of this structure plays an important role for wiping off the fouling. We have completed several tests on heat exchangers located at five different places with different working conditions. We found that the heat transfer coefficient declines first, and then keeps a constant value at about 0.54×10^{-4} m^2 K/W, and the thickness of the fouling layer remains almost unchanged when it reaches a certain level, as shown in Fig. 4.

In order to assess the fouling level of the nonlinear heat transfer device, we compared the fouling resistance of this device with that of other heat transfer devices, and found that the fouling resistance of this device is only one-third of the fouling resistance of the ordinary bare tube [11], and the antifouling ability of this heat transfer device is much better than that of the low rib tube, the screw tube and the spiral duct, etc. [12].

6. Conclusions

In the present work it is found that the vibration induced by the pulsation flow at the low flow velocity can significantly increase the convective heat transfer coefficient of the nonlinear heat transfer device. Compared with the average tube outside convective heat transfer coefficient of the fixed tube bundle, the average tube outside convective heat transfer coefficient of this device is improved by more than two times, while the fouling resistance is reduced by two-third.

The flow-induced vibration does not require additional energy. Although the vibration may increase the flow friction coefficient, it seems that the heat transfer coefficient on the heat surface is less dependent on the flow velocity. Therefore, the low flow velocity could be used which would result in low energy consumption.

The ordinary heat transfer enhancement devices demonstrate a good heat enhancement effect for the clear heat transfer surface, but when the fouling layer is formed, the heat transfer performance deteriorates rapidly. The heat transfer enhancement technology with the flow-induced vibration not only increases the convective heat transfer coefficient, but also decreases the fouling resistance. Therefore, the compound heat enhancement is achieved.

Acknowledgement

This research is supported by National Basic Research Program of China (Project No. 2007CB206900).

References

[1] D.S. Weaver, J.A. Fitzpatrick, A review of cross-flow induced vibration in heat exchanger tube arrays, J. Fluids Structures 2 (1998) 73–93.
[2] M.J. Pettigrew, C.E. Taylor, Two-phase flow-induced vibration: an overview, J. Pressure Vessel Technol. 116 (2) (1994).
[3] M.J. Pettigrew, C.E. Taylor, Damping of heat exchanger tubes in two-phase flow: review and design guidelines, J. Pressure Vessel Technol. 126 (4) (2004) 523–533.
[4] F. Michael, Flow-induced vibration in spiral finned gas tube bundle heat exchangers, American Society of Mechanical Engineers, Pressure Vessels and Piping Division (Publication), 460 (2003) 253–259.
[5] S.N. Choi, K.S. Yoon, T.S. Choi, An analytical method to predict fretting-wear damage in the double 90° U-bend tubes, International Conference on Nuclear Engineering, Proceedings, Fourteenth International Conference on Nuclear Engineering, 2006.
[6] M.K. Au-Yang, J.A. Burgess, Critical velocity of a non-linearly supported multi-span tube bundle, ASME Pressure Vessels Piping Div. Publ. PVP 19 (2006) 9–18.
[7] C.C. Gentry, W.M. Small, The ROD-baffle heat exchanger, ASM (Materials/Metalworking Technol. Ser.) (1982) 389–409.
[8] S. Krishnan, S. Kumar, Analysis of improved disc and doughnut configuration in shell and tube heat exchangers, Chem. Eng. Res. Design, Trans. Inst. Chem. Eng. A 72 (A5) (1994) 621–624.
[9] B. Peng, Q.W. Wang, et al., An experimental study of shell-and-tube heat exchangers with continuous helical baffles, J. Heat Transfer 129 (10) (2007) 1425–1431.
[10] Q.T. Zhou, S.Y. Huang, Heat Transfer Enhancement in Boiler and Heat Exchanger, China Water Power Press, 1991.
[11] G.F. Hewitt, Handbook of Heat Exchanger Design, Hemisphere Publishing Cooperation, New York, 1990.
[12] A.P. Watkinson, Fouling of augmented heat transfer tubes, Heat Transfer Eng. 11 (3) (1990) 57–65.